Title

Aqueous Diels–Alder reactions for thermochemical storage and heat transfer fluids identified using density functional theory

Journal

Journal of Computational Chemistry, 41(24)

ISSN

0192-8651

Authors

Spotte-Smith, Evan Walter Clark
Yu, Peiyuan
Blau, Samuel M
et al.

Publication Date

2020-09-15

DOI

10.1002/jcc.26378

Peer reviewed

Aqueous Diels–Alder reactions for thermochemical storage and heat transfer fluids identified using density functional theory

Evan Walter Clark Spotte-Smith[1], Peiyuan Yu[1], Samuel M. Blau[1], Ravi S. Prasher[1,2], and Anubhav Jain[1]

Correspondence to: Ravi S. Prasher (E-mail: rprasher@lbl.gov), Anubhav Jain (E-mail: ajain@lbl.gov)

[1] *Energy Technologies Area, Lawrence Berkeley National Laboratory, 1 Cyclotron Road, Berkeley, CA, 94720*

[2] *Department of Mechanical Engineering, 6141 Etcheverry Hall, MC 1740, University of California, Berkeley, CA, 94720*

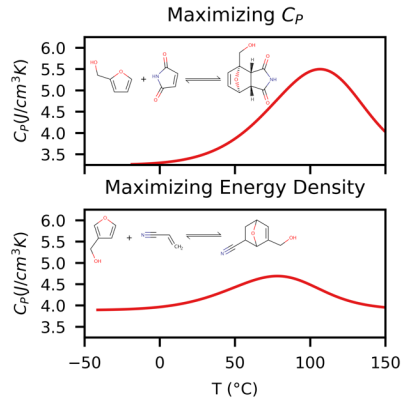

Graphical Abstract

In this work, density functional theory is employed to analyze the thermodynamic properties of aqueous Diels–Alder cycloaddition reactions to determine their suitability for thermochemical energy storage and heat transfer applications. Following a screening of 52 reactions for turning temperature and analysis of 60 additional functional group substitutions, several reactions emerge with exceptional thermal properties, enhancing water's heat capacity by as much as 30.5% and its total energy storage density by as much as 4.9%.

Keywords: Thermal storage, thermochemical, cycloaddition, Diels–Alder, density functional theory

Abstract

Thermal storage and transfer fluids have important applications in industrial, transportation, and domestic settings. Current thermal fluids have relatively low specific heats, often significantly below that of water. However, by introducing a thermochemical reaction to a base fluid, it is possible to enhance the fluid's thermal properties. In this work, density functional theory (DFT) is used to screen Diels–Alder reactions for use in aqueous thermal fluids. From an initial set of 52 reactions, four are identified with moderate aqueous solubility and predicted turning temperature near the liquid region of water. These reactions are selectively modified through 60 total functional group substitutions to produce novel reactions with improved solubility and thermal properties. Among the reactions generated by functional group substitution, seven have promising predicted thermal properties, significantly improving specific heat (by as much as 30.5%) and energy storage density (by as much as 4.9%) compared to pure water.

Introduction

Thermal fluids have many applications in thermal energy transfer and storage, playing a key role in heating, refrigeration, and power generation.[1] In an era of mounting concerns about energy use, their applications could be dramatically expanded to increase the efficiency of vehicles, improve heating and cooling in buildings, and recover waste heat in industrial processes.[2] The energy density of a thermal storage and transfer fluid is given by

$$E_S = \int_{T_{low}}^{T_{high}} C_p(T)dT \tag{1}$$

where C_p is the specific heat as a function of temperature T. Equation (1) shows that to achieve high volumetric or gravimetric energy density, high volumetric or gravimetric C_p is needed. To further increase the energy density, a wide working temperature range is needed.

A note on language: throughout this paper, we will use the terms "base fluid" and "thermal fluid". For our purposes, a "thermal fluid" is comprised of some "base fluid", which acts as a solvent, as well as any additional compounds dissolved in the base fluid. When we discuss the properties of a thermal fluid, we refer to the total properties, including the effects or contributions from the base fluid and the dissolved species.

Methods of Thermal Storage and Transfer

Conventional thermal fluids store and release sensible heat through the breaking and formation of noncovalent bonds such as hydrogen bonds (e.g., glycols), van der Waals forces (e.g., mineral oils), or electrostatic interactions (e.g., molten salts). The unusually high specific heat capacity of water originates from relatively strong and extended hydrogen bond networks

that dynamically form and break in response to changes in temperature.[3] Thus, water is usually the best choice for thermal fluid systems operating between approximately 5–95 °C. Another class of hydrogen bond-based fluids are glycols (e.g., ethylene glycol), which generally have specific heat capacities about one half that of water due to having fewer hydrogen bonds per unit mass. Because of the lower freezing point, mixtures of glycols and water are also commonly used as antifreeze. For example, a 1:1 mixture (by volume) of ethylene glycol and water can operate between approximately -30 °C to 105 °C, but with a reduced specific heat capacity (~3.6 J g^{-1} K^{-1}) compared to pure water. The high viscosity at low temperatures (e.g., 25 cSt at -20 °C) is also a disadvantage of glycol/water systems.[4] For systems that are not compatible with water or require higher operating temperatures, oils such as mineral, silicone, or synthetic oils are generally employed. These fluids, based on van der Waals interactions between their molecules, typically exhibit specific heat capacities less than one half that of water (~2 J g^{-1} K^{-1}).

Covalent bonds (typical bond strengths of hundreds of kJ mol^{-1}) can store vastly more energy than hydrogen bonds (10–30 kJ mol^{-1}) or van der Waals forces (< 5 kJ mol^{-1}). This makes thermochemical energy systems based on the formation and breaking of covalent bonds in the liquid phase attractively positioned to meet the increasing demand for thermal storage, as they can potentially deliver high volumetric and gravimetric energy densities.

To date, most thermochemical energy storage systems that have been developed are incompatible with use in thermal fluids, as they commonly rely on ionic solids, gases, or both.[5,6] However, a number of systems have been proposed that store thermal energy in covalent bonds via liquid-phase reactions, such as reactions between alcohols and aldehydes[7,8] and between amines and organic acids.[9]

In this manuscript, we explore a class of thermal fluids in which thermochemically reactive species are dissolved in a base fluid such as water. The dissolved species can reversibly react, forming and breaking covalent bonds in response to a change in temperature. As the bonds are broken, heat is absorbed, and as the bonds are formed, heat is released. In either direction, as the reaction occurs, it increases the effective specific heat capacity of the system, which also increases the energy storage density as defined in Equation (1). In a previous paper,[10] we derived the overall effective heat capacity of a thermal fluid containing reacting species as

$$C_P(T) = \frac{(\Delta H_{rxn})^2}{RT^2 K_{eq}(T)} \left(\frac{2c + \frac{1}{K_{eq}(T)}}{2\sqrt{\left(2c + \frac{1}{K_{eq}(T)}\right)^2 - 4c^2}} - \frac{1}{2} \right) + C_{P,fluid} \quad (2)$$

$$C_{P,fluid} = C_{P,base\ fluid} * \chi_{base\ fluid} + \sum_i C_{P,i} * \chi_i \quad (3)$$

where the summation in Equation (3) is over all reacting species present in the thermal fluid, c is the concentration of the reactants before the reaction has proceeded (no reactants have been converted to products), C_P is volumetric specific heat capacity, R is the gas constant (8.134 J

mol^{-1} K^{-1}), T is temperature in Kelvin, χ is the volume fraction of a given species, K_{eq} is the equilibrium constant of the reaction,

$$K_{eq} = e^{\frac{-(\Delta H_{rxn} - T\Delta S_{rxn})}{RT}} \quad (4)$$

ΔH_{rxn} is the reaction enthalpy,

$$\Delta H_{rxn} = H_{product} - \sum H_{reactant} \quad (5)$$

and ΔS_{rxn} is the reaction entropy,

$$\Delta S_{rxn} = S_{product} - \sum S_{reactant} \quad (6)$$

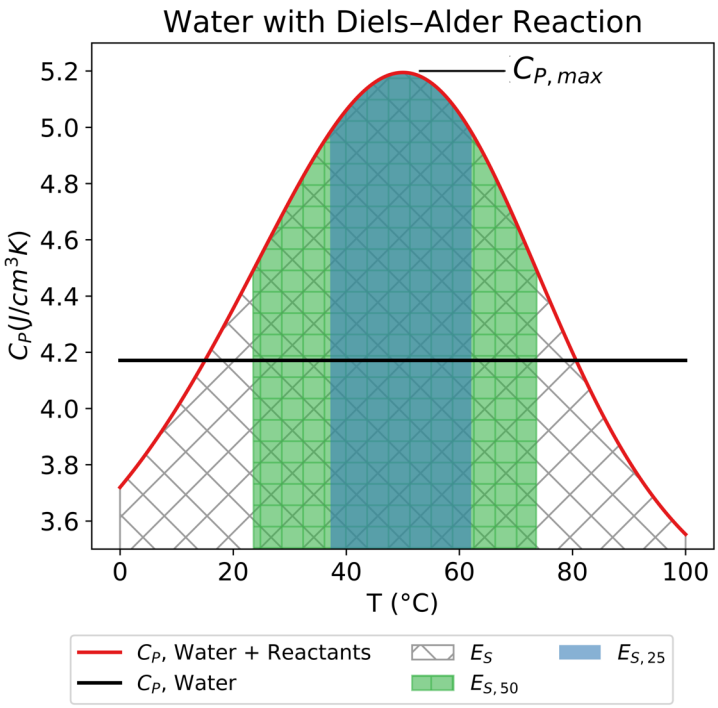

Figure 1: A schematic depiction of enhanced heat capacity and energy storage density (integrated heat capacity over temperature) for a hypothetical thermal fluid comprised of Diels–Alder reactants dissolved in water. The shaded areas under the heat capacity curve indicate the total volumetric energy storage density E_S (gray diagonal cross-hatch), optimal volumetric energy storage density over a 50-degree range $E_{S,50}$ (green with vertical and horizontal cross-hatch), and the optimal volumetric energy storage density over a 25-degree range $E_{S,25}$ (blue). The maximum volumetric heat capacity $C_{P,max}$ is also indicated. For comparison, the volumetric heat capacity of water is also included.

Figure 1 depicts the effective volumetric heat capacity for a thermal fluid comprised of Diels–Alder reactants dissolved in water. The area under the curve represents the volumetric energy storage density. We calculate energy storage density in three ways. The energy storage density over the entire working temperature range (0–100 °C), represented in the figure by the gray cross-hatch, is E_S. Because some reactions may demonstrate heat capacity enhancement over a narrow temperature range, we also calculate energy density over a 50°C window within the working temperature range of water ($E_{S,50}$, the green region) and over a 25°C window within

the working temperature range of water ($E_{S,25}$, the blue region). The temperature windows for $E_{S,50}$ and $E_{S,25}$ depend on the specific reaction; in each case, the temperature ranges are chosen in order to maximize the energy density enhancement of the reaction. In most cases, these windows are centered near the maximum effective heat capacity, $C_{P,max}$.

From Equation (2), it can be seen that the form of the heat capacity enhancement is closely related to both the concentration of the reactants in the base fluid as well as the reaction thermodynamics. Importantly, the maximum of the heat capacity enhancement occurs near the turning temperature of the reaction T^*, where

$$T^* = \Delta H_{rxn} / \Delta S_{rxn} \tag{7}$$

The turning temperature defines the point at which the reactants and the products of the reaction are equally thermodynamically favorable ($\Delta G_{rxn} = 0$) and is related to the thermal reversibility of a reaction. A turning temperature within the working temperature range of the base fluid is highly desirable for a thermal fluid, as it would imply that the reaction can both release (through the forwards reaction) and store (through the reverse reaction) useful quantities of energy within that working range. Conversely, if the turning temperature of a reaction is significantly outside of the working range of the base fluid, that reaction will be incompatible with the base fluid for thermal storage or transfer applications. Because either the products or the reactants are favored throughout the working range, a reaction with a turning temperature significantly outside of the working temperature range of the base fluid would have a limited ability to convert heat to chemical bonds or vice versa.

Diels–Alder Reactions for Aqueous Thermochemical Energy Storage and Transfer

As a demonstration of the potential of thermal fluids containing thermochemically reactive species, we consider Diels–Alder reactions dissolved in water. Water was chosen as the base fluid because of its exceptionally high specific heat capacity. Diels–Alder reactions[11] are [4 + 2] cycloaddition reactions; the two reactants (one of which, the diene, has two conjugated double bonds and the other of which, the dienophile, has a double or triple bond) react to form a six-member ring. As a result of a Diels–Alder reaction, three π bonds are broken, and two σ bonds and one π bond are formed. These reactions have been widely used by synthetic chemists since their discovery, as the reaction mechanism is highly predictable and often simple to perform.[12]

Diels–Alder reactions have previously been proposed as thermal energy conversion materials.[13,14] These reactions are attractive because they can attain relatively high reaction enthalpies, ΔH_{rxn},[15] which allows for high energy density. Moreover, because of the high entropy change ΔS_{rxn} associated with cycloaddition, the turning temperature T^* can often be low enough to be within the liquid phase range of water.[16] Thus, we expect that some Diels–Alder reactions will be reversible at moderate temperatures and that thermal fluids based on these reactions will elevate effective heat capacity and energy storage density within the working temperature range of water. Despite their potential, few efforts have been made since the initial investigations to further explore this family of reactions in thermal fluid applications.[17]

Computational Screening for Thermochemical Reactions

In order to identify promising reactions for applications in thermal energy storage and transfer, we perform a computational screening of Diels–Alder reactions. Sparks and Poling[18] noted that because the properties of interest for thermal energy storage and transfer were difficult to predict, especially the reaction thermodynamics and related quantities, it was difficult to identify appropriate reactions for use in thermal fluids. However, modern high-throughput computational calculation and screening techniques, relying on density functional theory, make selection of materials in even vast search spaces tractable.[19,20,21,22]

A number of screening studies have previously been performed to identify appropriate thermochemical energy storage materials for a variety of applications. A recent review by Dizaji and Hosseini[23] provides an excellent summary. Recent work by Kiyabu et al.[24] has leveraged high-throughput first-principles calculations to screen hydration reactions for thermochemical storage applications. To our knowledge, such a computational screening approach has not been applied to liquid-phase thermochemical reactions generally, nor specifically to Diels–Alder reactions for thermochemical storage applications.

In our screening, we computationally study the thermodynamics of aqueous Diels–Alder reactions to identify candidates for efficient thermochemical storage. We analyzed an initial test set of 52 Diels–Alder reactions through density functional theory (DFT) calculations, generating predicted values of reaction enthalpy, entropy, and turning temperature. We then screened these reactions based on their compatibility with water in terms of aqueous solubility and turning temperature. From this test set, we selected several reactions which we then selectively modified by functional group substitution in order to improve the solubility, thermodynamic properties, and thermal properties of the reactions.

Methods

Test Set Generation

Figure 2 depicts the sequential screening process used to generate the test set. Candidate reactions (and the component molecules involved in those reactions) were obtained from the Reaxys database.[25] A query was performed for reactions labeled “Diels–Alder”; the Diels–Alder reactions were then further filtered to produce a set which had a yield ≥ 90%, which proceeded in a single step (to simplify experimental synthesis), and which had two reactants and a single product. From this, 1,821 reactions were obtained. Of these 1,821 reactions, 153 had been performed in an aqueous solution (defined as any solution including water) in the literature. Further filtering was conducted to remove duplicate reactions, reactions involving ionic species, and reactions in which additional species – dissolved salts - were required. One reaction (benzaldehyde/phenylacetylene) was removed from consideration because, though labeled as a Diels–Alder reaction, it is not a cycloaddition reaction.

After this filtering, 66 reactions remained. To limit the computational resources demanded, a time limit of 300 CPU-hours was placed on all opt-freq-sp(solv) calculations

(workflow described later); calculations for 13 reaction products failed to complete within that time limit. One reaction (furan/maleimide *endo*) was removed from primary consideration because the *exo* Diels–Alder reaction is typically thermodynamically preferred and so is most relevant to the present thermodynamic analysis (results for the furan/maleimide *endo* reaction are presented in the Supporting Information). The final test set thus consisted of 52 reactions.

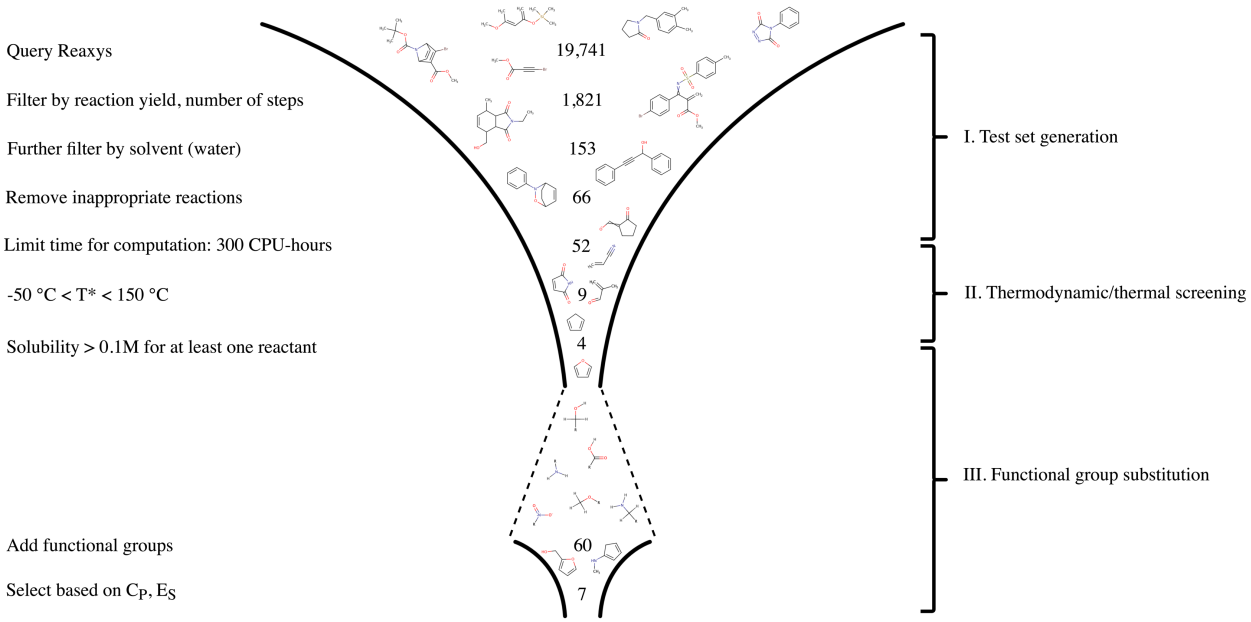

Figure 2: A "funnel" depicting the selection process for reactions for this study. From an initial 19,741 reactions obtained from Reaxys, a test set of 52 reactions was obtained (I. Test set generation). These 52 reactions were analyzed using DFT, as described in Calculation Workflows and were screened based on their calculated properties, eventually leading to four reactions with promising properties (II. Thermodynamic/thermal screening). Finally, these four reactions were selectively modified by functional group substitution (see "Functional Group Substitutions" in Methods), leading to a new pool of 60 reactions, of which seven have been identified as promising candidates for future study (III. Functional group substitution).

Calculation of Molecular and Reaction Properties

Equations (1) and (2) are the metrics that determine the potential utility of a thermal fluid. For a given thermal fluid including some reactive species, these equations rely on the thermodynamics of the reaction as well as the chemical composition of the thermal fluid.

The thermodynamic properties of individual molecules were calculated directly using DFT (see Calculation Workflows below for details). Specifically, the solvation-corrected internal energy (E_{solv}), enthalpy (H_{vac}), and entropy (S) were calculated for each molecule in the test set. The overall enthalpy of each molecule was then calculated as

$$H = H_{vac} + H_{solv} \approx H_{vac} + E_{solv} \quad (8)$$

and these values of H and S were used to calculate the reaction enthalpy via Equation (5) and reaction entropy via Equation (6). The turning temperature for each reaction was then calculated using Equation (7).

The concentration c of the reacting species is limited by the solubility of the species in water; that is, $0 \leq c \leq c_{max}$, where c_{max} is the maximum aqueous solubility of the reaction. The solubility of the reaction as a whole is limited by the lowest solubility among its reacting species. To determine c_{max}, the aqueous solubility of each reacting species was calculated using the U.S. Environmental Protection Agency's EPI Suite.[26] EPI Suite calculations are based on quantitative structure-property relations (QSPR) models. They require no input parameters other than the Simplified Molecular Input Line Entry System (SMILES) strings[27] of the molecules of interest, making them easily applicable to a wide range of molecules. In addition to the aqueous solubility, the boiling point of each molecule was calculated using EPI Suite. Note that all predicted normal boiling points were calculated without considering a solvent; the actual boiling points of the molecules in water may differ significantly from the values for the pure molecules.

Some approximations are made in the application of Equations (2) and (3) in the present study. The sensible specific heat capacity of the thermal fluid $C_{P,fluid}$, which accounts for the contributions of the base fluid and the organic reactants, is taken to be independent of temperature. The volumetric specific heat capacity of the base fluid (water), $C_{P,base\ fluid}$, is set to a constant value of 4.171 J cm^{-3} K^{-1} (the volumetric specific heat capacity of water at 25°C), and the volumetric specific heats of all organic reactants $C_{P,i}$ are assumed to be 2.0 J cm^{-3} K^{-1}. This latter approximation is necessary because the specific heat capacities of many of the molecules studied here have not been reported in the literature. Because the densities of many of the organic molecules studied here have also not been measured by experiment, the volume fractions χ_i are calculated based on the assumption that all molecules have the same density as water. Constant χ_i values are used, with the value at 25°C being chosen for each species. The maximum aqueous solubility c_{max} is also taken to be independent of temperature; the value at 25°C, as calculated in EPI Suite, is used throughout the working temperature range of water. It should be noted that this is not generally the case (solubility is likely to vary with temperature), and that this method will generally overestimate the solubility at low temperatures and underestimate solubility at high temperatures.

Calculation Workflows

Any necessary modifications to the studied molecules - converting a 2D to a 3D structure, adding implicit hydrogens to the structure, and performing a preliminary geometry optimization - were completed using pymatgen[28] and OpenBabel Python libraries openbabel[29] and pybel.[30] After pre-processing, the atomic and electronic structures of each molecule were calculated using the Q-Chem DFT code[31] using one of two workflows, a coarse workflow we call "opt-freq-sp(solv)" and a more accurate workflow we call "opt(solv)-freq(solv)".

In the coarse opt-freq-sp(solv) workflow, molecular geometries were optimized using the ωB97X-D functional[32] with a 6-31G(d)[33] basis set. ωB97X-D was chosen because it has been shown to have relatively low error when predicting the reaction energies of Diels–Alder

reactions.[34] These optimized geometries were then fed into a vibrational frequency calculation using the same functional and basis, yielding the molecular enthalpy and entropy. In cases where the initial optimized geometry yielded imaginary frequency modes (indicating a transition state or other non-equilibrium geometry), the optimization and vibrational frequency calculations would be repeated following a perturbation of the molecule geometry. A single-point energy calculation was made with a larger basis set (6-311++G(d,p));[35] these calculations also used the IEF-PCM solvation model[36] with water (dielectric constant $\varepsilon = 80.4$) as the solvent in order to correct for the effect of solvation on the molecule. All basis sets were taken from the Extensible Computational Chemistry Environment Basis Set Database, Version 1.0,[37] as implemented in Q-Chem.

After initial calculation using the coarse method described above, some exceptional cases with appropriate thermodynamic properties and reasonable physical properties (including boiling point and aqueous solubility) were re-calculated using a more accurate method, opt(solv)-freq(solv). Using the vacuum-optimized geometry as a starting point, the molecules were re-optimized and the frequencies were re-calculated. Both geometry optimization and frequency calculations were made using ωB97X-D/6-311++G(d,p) in solvent. The SMD method,[38] which combines the electrostatic contribution from IEF-PCM with a term based on short-range interactions, was chosen as the solvation method. Because solvation and a large basis set were used for optimization and vibrational frequency calculations, no single-point calculation was needed for the accurate workflow. Again, in the case of imaginary frequency modes, the molecules would be repeatedly perturbed and re-optimized.

After preliminary tests on small molecules, the opt-freq-sp(solv) and opt(solv)-freq(solv) workflows were automated using atomate,[39] a library that builds off of the FireWorks dynamic workflow system[40] to construct high-level computational processes for materials science. We used atomate to automatically execute the computational workflows that prepare input files for DFT calculations, parse outputs, and store results on a per-molecule and per-reaction basis sensibly in a database.

Functional Group Substitutions

As described in "Test Set Generation", the reactions chosen for this study were taken from a database that is based on the available literature. This approach ensures that the reactions studied are chemically valid, but these previously studied reactions may not be the most appropriate for the present application. Specifically, many of the molecules studied have low boiling points and are insoluble in water. Further, for many of the reactions studied, the turning temperature is inappropriate for use in water (see "Selecting Reactions for Substitution" below). For these reasons, it is desirable to generate new reactions to improve on these deficiencies. Here, a simple method to generate reactions not in the test set using functional group substitution is described.

The most promising reactions from the initial test set were those that had turning temperatures within or close to the working temperature range of water and that were primarily limited in solubility by only one reacting molecule. In other words, the solubility of one reactant

was low, and the solubility of the other reactant was reasonably high. These promising reactions were modified in order to improve or tune the predicted solubility, boiling point, and thermodynamic properties. In each of these modifications, a hydrogen atom in one of the reactant molecules was removed and replaced with a functional group. A hydrogen atom at the corresponding site in the product molecule was then removed and replaced by the same functional group. The functional groups considered were carboxyl (COOH), methoxy (OCH_3), nitro (NO_2), methylamine (CH_2NH_2), amine (NH_2), and hydroxymethyl (CH_2OH). These functional groups were chosen because they are polar and thus could be expected to improve aqueous solubility. The addition of any functional group was expected to increase the boiling point, as larger molecules typically boil at higher temperatures than smaller molecules.

In order to automatically facilitate this functional group substitution, the reactant and product molecules were represented as undirected graphs using pymatgen and the Python networking library networkx,[41] with nodes representing atoms and edges representing bonds between those atoms. Subgraph isomorphisms between the reactant graph and the product graph were constructed such that the bond characteristics (bond strength, bond length, etc.) were ignored, but the atomic species of each node was matched. After creating an atom-to-atom mapping using this subgraph isomorphism, the graphs were then modified by eliminating a selected hydrogen node and replacing it with a new subgraph representing the functional group of interest. Changes to the graph were reflected in changes in the molecule geometry, with initial guesses for the locations of each atom in the added functional group being taken from pre-tabulated data in pymatgen.

It should be noted that the functional group substitutions considered here are limited to perform a single substitution on a single reactant molecule. It would in principle be possible to perform substitutions on both reactants simultaneously or to perform multiple substitutions on the same reactant using a similar methodology to the one described here. However, this would dramatically increase the number of reactions considered, especially for reactions involving large molecules with many possible sites for substitution. Furthermore, it is possible that some of the reactions initially considered as unpromising could be improved through the use of substitutions. For reasons of computational cost, multiple substitutions have not been considered here, and all substitutional studies focus only on initially promising reactions, though such substitutions should be considered in subsequent studies, as they could yield novel reactions with useful properties.

Screening and Selection Considerations

In the preliminary screening stage, reactions with appropriate turning temperature T^* and maximum aqueous solubility c_{max} were sought. These factors determine the magnitude of the thermochemical heat capacity enhancement, as well as the temperature range in which that enhancement occurs. The reactions that passed through this preliminary screening were subjected to functional group substitution in order to tune these properties and produce reactions with more practical thermal properties (see “Functional Group Substitution”).

An ideal reaction would have T^* within the working range of water (0–100 °C). These reactions could reasonably be expected to enhance the specific heat capacity of water, storing and releasing useful quantities of thermochemical heat. For the preliminary screening, this temperature was expanded to -50–150 °C for three reasons. First, some error in the calculated turning temperature was anticipated for the coarse opt-freq-sp(solv) workflow. A turning temperature that is predicted to lie outside of the working range of water at a lower level of theory might actually be within the working temperature range when recalculated at a higher level of theory or in experiments. Second, some gains in heat capacity and energy density could be seen even if the turning temperature is outside of the working temperature range by a small amount. Finally, substitutions onto candidate molecules can help tune the turning temperature of the original reaction. Reactions with turning temperatures slightly outside the working range of water were retained in this stage of the screening so that the effects of functional substitution could be explored in the next stage.

The functional group substitution method used in this work is limited to only substitute a single functional group onto a single reactant. Such a functional group substitution would improve the solubility of that single reactant and the substituted product molecule. Thus, if the solubility of the reaction is primarily limited by only one reactant, functional group substitutions could be highly effective for improving reaction solubility. However, if both reactants of a reaction have low aqueous solubility, then the reaction solubility could still be significantly limited by the reactant that did not experience a substitution. Therefore, reactions were selected for which the solubility of at least one reactant was greater than or equal to 0.1M.

Reactions generated by functional group substitution were selected on the basis of their thermal properties, namely the maximum effective heat capacity ($C_{P,max}$) and energy storage density (E_S, $E_{S,25}$, or $E_{S,50}$), as these are the primary quantities of interest for practical thermal fluids. To maximize each of these quantities for a given reaction, brute-force optimizations were performed to determine an optimal reaction concentration $0 \leq c \leq c_{max}$. For $E_{S,25}$ and $E_{S,50}$, the optimal temperature ranges were also determined separately for each reaction considered. Reactions were then selected that demonstrated high effective heat capacity or energy storage density.

Results

Selecting Reactions for Substitution

The calculated thermodynamic properties of the 52 reactions in the initial screening set are plotted in Figure 3. It can be seen that the majority of the reactions studied have turning temperatures above the boiling point of water and are thus inappropriate for use in an aqueous system. However, nine reactions have predicted turning temperatures within an expanded temperature range (-50–150 °C) close to the working temperature range of water. These reactions, hereafter the “potentially reversible reactions”, are located within the black box in Figure 3; they are also listed in Table 1. The effective heat capacities of these reactions as a function of temperature, calculated according to Equation (2), are plotted in Figure 4; tables with

the thermodynamic and thermal properties of the potentially reversible reactions are provided in the Supporting Information. We note that these values are calculated with the less accurate opt-freq-sp(solv) workflow.

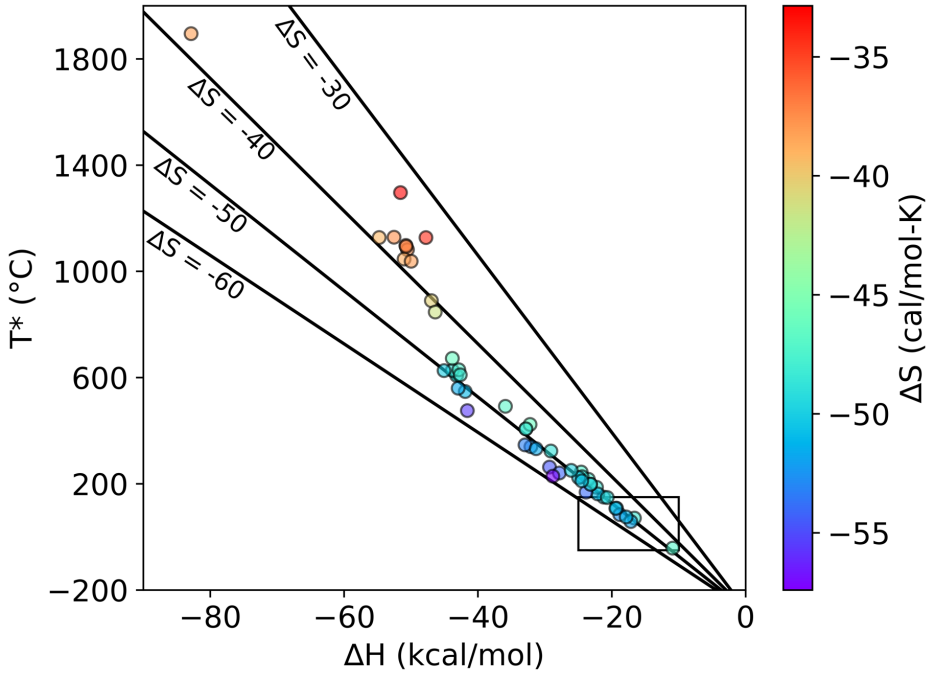

Figure 3: Predicted turning temperature T^* plotted against enthalpy ΔH_{rxn} for all reactions in the test set, calculated using opt-freq-sp(solv). The lines denote constant reaction entropy ΔS_{rxn}; reaction entropy is also represented by the color of the points. The box contains all reactions with turning temperature in the range (-50–150 °C), the "potentially reversible reactions".

Table 1: Names and reaction diagrams for potentially reversible reactions. Numbers will be used in subsequent discussion.

Number	Name	Diagram
(1)	cyclopentadiene/crotonaldehyde	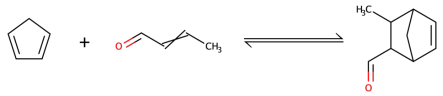
(2)	cyclopentadiene/3-nitrocoumarin	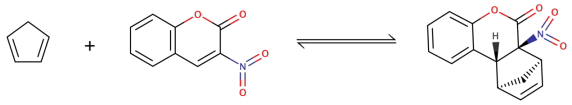
(3)	cyclopentadiene/3-(4-nitrophenyl)-2-propenal	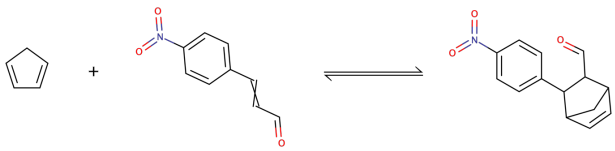
(4)	cyclopentadiene/2-methylpropenal	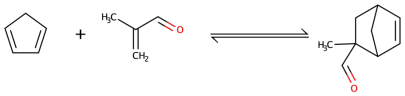

(5)	cyclopentadiene/menadione	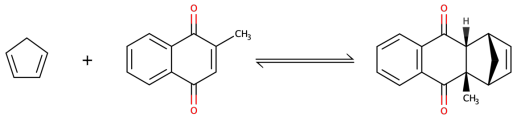
(6)	cyclopentadiene/3-phenyl-propenal	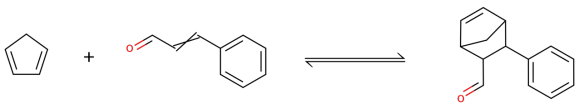
(7)	cyclohexadiene/nitrosobenzene	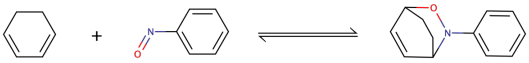
(8)	furan/acrylonitrile	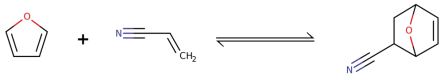
(9)	furan/maleimide *exo*	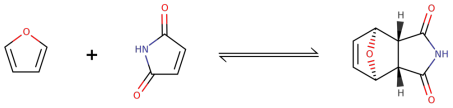

Both solubility and boiling point limit the utility of most of the potentially reversible reactions (see Supporting Information for detailed results). The solubility of the reacting species in water tends to be low, in many cases less than 0.01M. This is unsurprising, given the nature of the species (in many cases, cyclic or even multicyclic organic molecules with relatively few, if any, polar groups). These extremely low-solubility systems are expected to exhibit minimal energy storage gains. In Figure 4, the modeled heat capacity curves for the reactions with the lowest aqueous solubility – (2), (3), (5), and (6) – are barely visible, indicating near-zero heat capacity enhancement; reactions with moderate solubility, such as (9), show noticeable gains in heat capacity. Additionally, several of the reacting molecules, notably furan (H_4C_4O) and cyclopentadiene (H_6C_5), have boiling points significantly below that of water (noted in Figure 4 as black "x" marks), potentially reducing the working range of the system if the boiling point of the solution is similarly low.

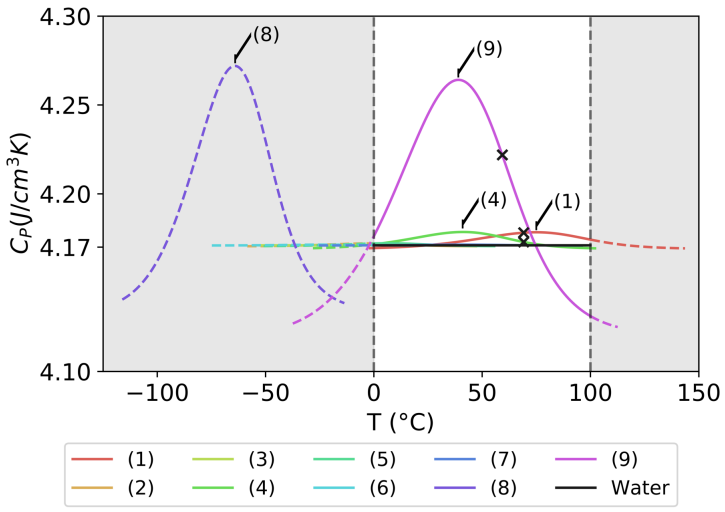

Figure 4: Predicted effective specific heat capacities $C_p(T)$for aqueous thermal fluids containing the potentially reversible reactions with T^* in range (−50, 150) °C. The reactions are labeled according to the numbering in Table 1. All curves are plotted from T_{low} to T_{high}, where T_{low} is the temperature at which the solution is predicted to be 1% reactant, and T_{high} is the temperature at which the solution is predicted to be 99% reactant. For all curves, the reaction concentration is equal to the maximum solubility of the reaction, c_{max} (based on the solubility of the least soluble molecule involved in the reaction). Dashed lines in the dark area indicate regions outside the working temperature range of water (light area). Curves that lie outside of the working range could not be expected to proceed in water but are shown for completeness. Black "x"s indicate the lowest predicted boiling point of any of the reacting species of a reaction, if this value is below 100 °C. It is assumed that no boiling occurs below the boiling point of water. Thermodynamic values are based on the less accurate opt-freq-sp(solv) workflow.

Modified Reactions

Of the reactions with an acceptable turning temperature, only in the furan/acrylonitrile system (8) and the furan/maleimide system (9) did all components (reactants and products) of the reaction have solubilities greater than 0.1 M (in both of these systems, the solubility is limited by furan). In several other reactions, namely cyclopentadiene/crotonaldehyde (1) and cyclopentadiene/2-methylpropenal (4), the solubility is strongly limited by the diene (cyclopentadiene); the solubilities of the dienophiles in reactions (1) and (4) are greater than 0.1 M. In an attempt to tune the properties of these reactions, increasing the boiling points and solubilities of furan and cyclopentadiene, additional candidate reactions were generated from reactions (1), (4), (8), and (9) by substituting functional groups onto the diene and the product molecules. This process is described in Methods and is further illustrated in Figure 5 for the addition of an amine group to site 2 of furan in the furan/maleimide *exo* reaction. In addition to improving solubility and increasing boiling point, these functional groups were expected to affect the reaction thermodynamics of (1), (4), (8), and (9), potentially affecting the turning temperature. Note that substitutions onto cyclohexadiene/nitrosobenzene (7) were also attempted, but as none of these substitutions led to significant enhancements in heat capacity or energy density, they have been excluded from subsequent analysis (these results are reported in the Supporting Information).

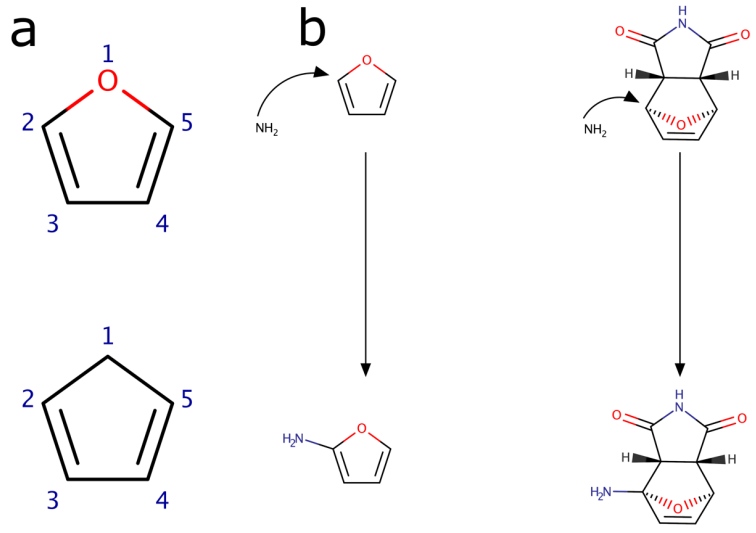

Figure 5: (a)From top to bottom, mapping of furan and cyclopentadiene positions; (b) depiction of the generation of 2-aminofuran and the 2-aminofuran/maleimide *exo*-product from the initial reactant and product. In this study, substitutions were made onto sites 2 (symmetrically equivalent to site 5) and 3 (symmetrically equivalent to site 4) of furan and onto sites 1, 2

(symmetrically equivalent to site 5) and 3 (symmetrically equivalent to site 4) of cyclopentadiene. The functional group, in this case an amine group, replaces a hydrogen atom at the site indicated by the curved arrow in both the reactant and the product.

We also analyzed substituted reactions with modified dienophiles, including on acrylonitrile for reaction (8) and maleimide for reaction (9). These substituted reactions generally led to small improvements in heat capacity or energy density, since the overall reaction solubility was still limited by the relatively insoluble furan. Furthermore, reactions with substituted maleimide and acrylonitrile molecules frequently resulted in turning temperatures significantly outside the desired temperature range. The full results of these substitutions are included in the Supporting Information.

The thermodynamic properties of the reactions generated by selective functional group substitution were calculated using the coarse opt-freq-sp(solv) workflow. The predicted effective heat capacity curves for these modified reactions are plotted in the first three columns of Figure 6 (see the Supporting Information for predicted aqueous solubility values as well as normal boiling points for the furan derivatives). Among the substitutions modeled using opt-freq-sp(solv) workflow, several emerge as having favorable properties for aqueous thermochemical storage. Reactions 2-methylaminocyclopentadiene/crotonaldehyde (10), 2-aminocyclopentadiene/crotonaldehyde (11), 2-methylaminocyclopentadiene/2-methylpropenal (12), 2-aminocyclopentadiene/2-methylpropenal (13), 2-aminofuran/maleimide, and 2-hydroxymethylfuran/maleimide (16) are predicted to achieve high effective heat capacity with a turning temperature within the working temperature range of water. 1-aminocyclopentadiene/2-methylpropenal, 2-hydroxymethylfuran/acrylonitrile (14), 3-hydroxymethylfuran/acrylonitrile (15), 2-aminofuran/acrylonitrile, and 3-hydroxymethylfuran/maleimide *exo* also demonstrate high heat capacity, but with turning temperatures slightly outside of the working temperature range. We analyzed these reactions, as well as the unmodified reactions (1), (4), (8), and (9) with the more accurate opt(solv)-freq(solv) workflow in order to better understand their thermodynamic and thermal properties. The effective heat capacity curves for these reactions as calculated with the more accurate opt(solv)-freq(solv) workflow can be seen in the fourth column of Figure 6. This column represents the most accurate results calculated in this paper on the final set of reactions of interest.

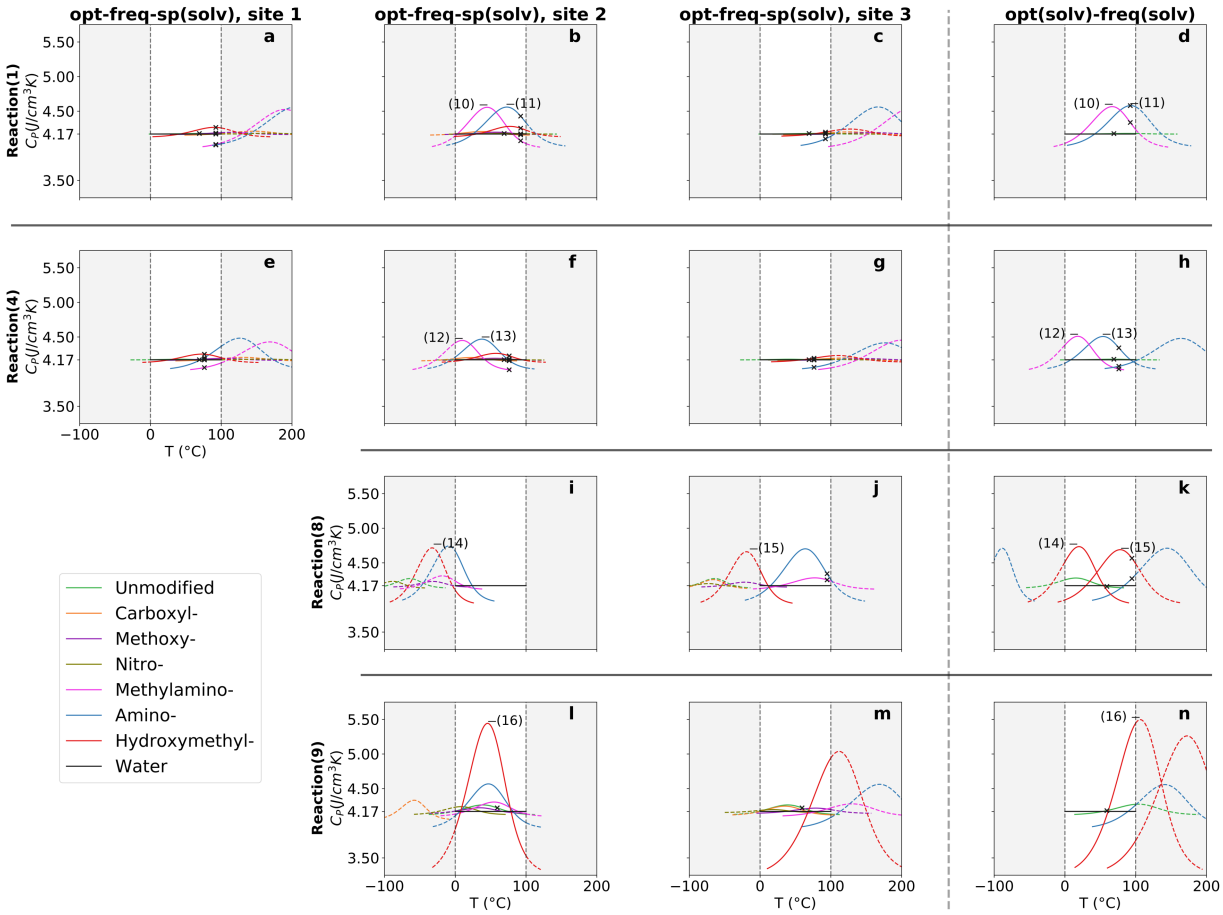

Figure 6: Modeled heat capacities (including aqueous solvent) over the temperature range -100–200 °C for cyclopentadiene/crotonaldehyde (1) (a-d), cyclopentadiene/2-methylpropenal (4) (e-h), furan/acrylonitrile (8) (i-k), and furan/maleimide *exo* (9) (l-n) reactions with diene sites modified. Reactions depicted in the first column (a, e) had the 1-site modified, reactions in the second column (b, f, i, l) had the 2-site modified, and reactions in the third column (c, g, j, m) had the 3-site modified. Calculations for these first three columns were performed with the coarse opt-freq-sp(solv) workflow. Some reactions were selected for more accurate calculation with the opt(solv)-freq(solv) workflow; these calculations are depicted in the fourth column (d, h, k, n). For all curves, the reaction concentration is equal to the maximum solubility of the reaction, c_{max} (based on the solubility of the least soluble molecule involved in the reaction). Dashed lines indicate regions outside the working temperature range of water (light area); curves that lie outside of the working temperature range could not be expected to proceed in water. Black "x"s indicate the lowest predicted boiling point of any of the reacting species of a reaction when this value is below 100 °C.

Figure 6 illustrates the effect of functional group substitution on the thermodynamic and thermal properties of Diels–Alder reactions. The predicted aqueous solubility of the diene molecules (and, thus, the reactions) increased for all functional group substitutions. The most significant solubility improvements occurred with additions of methylamine, amine, and hydroxymethyl groups, increasing the aqueous solubility of the diene by several orders of magnitude. This increase in solubility is the main factor driving the improved heat capacities seen in Figure 6. However, the reaction thermodynamics also changed as a result of functional group substitutions. For a given unsubstituted reaction, the turning temperature of the substituted reactions can vary widely as a result of different choices of functional group and even substitution site. The site-specificity is especially pronounced for the amine, carboxyl, and

methylamine substitutions, where the choice of position frequently modifies the turning temperature by more than 75 °C. The entropy of reaction changed little (at most 13.5% for 2-carboxylfuran/acrylonitrile), but in most cases did become slightly more negative with functional group substitution. On average, ΔS_{rxn} changed by -0.704 cal mol^{-1} K^{-1} following functional group substitution, an average change of 1.5%. Reaction enthalpy is more tunable; ΔH_{rxn} changed by as much as 67.4% for 3-methylaminofuran/acrylonitrile and on average changed by -1.397 kcal mol^{-1}, or 8.8%. As specific heat and energy density are dependent on ΔH_{rxn} and concentration c, our results suggest that the thermal properties of Diels–Alder reactions can be tuned by appropriate functional group substitutions.

We note that dissolving more of the reacting species in water is not always beneficial. Because water has a higher sensible heat capacity that organic molecules in general, dissolving the organic molecules actually depresses the base sensible heat capacity (Equation (3)). The thermochemical heat capacity enhancement due to the reaction (Equation (2)) must overcome this reduction in sensible heat capacity for the net effect to be beneficial. For energy density (Equation (1)), which considers a range of temperatures, a net benefit in one temperature region must overcome a net deficit in other temperature regions for the reaction to be beneficial overall. For some reactions shown in Figure 6, there was no available concentration at which the energy density could overcome the loss in sensible heat capacity.

Seven of the substituted reactions analyzed using the more accurate opt(solv)-freq(solv) workflow, reactions (10)-(16), show great promise for use in thermal storage and transfer applications. These reactions are listed and depicted in Table 2. Their predicted thermodynamic properties are also listed in Table 2, and their thermal storage properties are given in Table 3. The utility of these reactions for thermal storage applications varies depending on the application of interest. For low-temperature applications (T < 50°C), reaction (14) offers the greatest gains in energy storage density, at 10.0% over the 50°C range. In the upper half of the working temperature range (50°C < T < 100°C), reactions (15) (10.4% gains) and (16) (11.9% gains) are most promising, though for reaction (15) boiling may still present problems. Over a narrower temperature range (75–100°C), reaction (16) displays especially high energy storage density, with a 22.3% improvement over pure water, and with low risk of boiling (predicted T_b > 100°C). Reactions (10) and (15) have the highest predicted energy storage densities over the entire working temperature range (improving over the base fluid by 4.1% and 4.9%, respectively), and reaction (16) has by far the highest effective heat capacity, at 5.445 J cm^{-3} K^{-1} (a 30.5% improvement over the base fluid).

The 2-hydroxymethylfuran/maleimide *exo* reaction (16) significantly increases the effective heat capacity of water through the introduction of a thermochemical mechanism. Previously, Sparks and Poling[18] modeled a thermal fluid based on the 2-methylfuran/maleic anhydride Diels–Alder reaction in a 7M solution with 1,4-dioxane. The effective heat capacity for this system was modeled to be as high as 7.37 J cm^{-3} K^{-1}. The 2-methylfuran/maleic anhydride reaction was not considered in our study because it has not proceeded in water in the literature. While the heat capacity obtained by Sparks and Poling is higher than any reaction considered here, including (16), the reactions identified here benefit from water solubility. Water

has a marginally wider working temperature range than dioxane (which is only liquid between 11.8–101.1 °C). More importantly, water benefits from a lower cost when compared to dioxane, and it is already commonly used and readily available as a thermal fluid. This means that in general, the reactions identified here could more readily be applied to existing systems.

Table 2: Reaction diagrams, predicted thermodynamic properties, solubility c_{max} (based on the solubility of the least soluble molecule involved in the reaction), and boiling point T_b (based on the lowest normal boiling point among the reactants of a given reaction) for several promising substituted reactions, based on values from the opt(solv)-freq(solv) workflow and EPI Suite.

Reaction	**Base Reaction**	**Diagram**	**ΔH_{rxn} (kcal mol^{-1})**	**ΔS_{rxn} (cal mol^{-1} K^{-1})**	**T^* (°C)**	**c_{max} (M)**	**T_b (°C)**
(10)	(1)	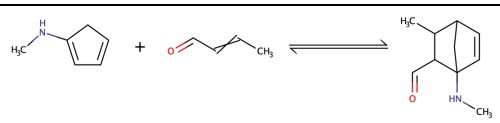	-18.241	-51.591	80.42	0.592	92.35
(11)	(1)	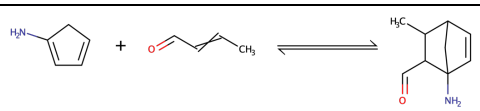	-19.589	-51.441	107.66	0.592	92.35
(12)	(4)	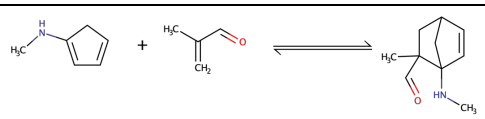	-16.218	-53.096	32.29	0.454	76.22
(13)	(4)	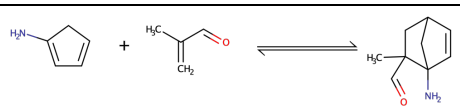	-17.897	-52.152	70.03	0.454	76.22
(14)	(8)	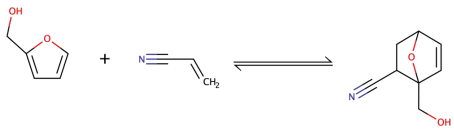	-15.426	-51.289	27.62	0.854	94.65
(15)	(8)	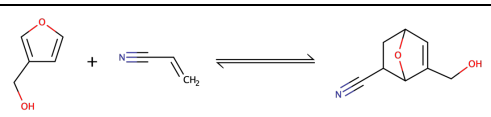	-18.008	-49.890	87.80	0.854	94.65
(16)	(9)	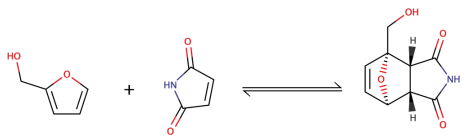	-20.446	-54.372	102.90	2.173	170.16

Table 3: Predicted thermal properties (heat capacity, energy density) of several promising substituted reactions. Three values of energy density are given: E_S, the energy density over the entire working temperature range of water (0-100 °C); $E_{S,25}$, the maximum energy density over a 25-degree range, and $E_{S,50}$, the maximum energy density over a 50-degree range. Where appropriate, the temperature range is given. The proportional gain, or gain, for a quantity is defined as the difference between the

quantity in the thermal fluid and the quantity in pure water, divided by the quantity in pure water. Except where noted, all calculations are made using the maximum solubility c_{max} as the concentration.
[a] c = 0.572 mol L^{-1} for this value

Reaction	$C_{P,max}$ (J cm^{-3} K^{-1})	Gain (%)	E_S (MJ L^{-1})	Gain (%)	$E_{S,25}$ (MJ L^{-1})	Gain (%)	Temp. Range (°C)	$E_{S,50}$ (MJ L^{-1})	Gain (%)	Temp. Range (°C)
(10)	4.566	9.5	0.4344	4.1	0.1136	9.0	55.26–80.26	0.2246	7.7	39.47–89.47
(11)	4.581	9.8	0.4272	2.4	0.1139	9.2	75.00–100.00	0.2229	6.9	50.00–100.00
(12)	4.510	8.1	0.4234	1.5	0.1121	7.5	3.95–28.95	0.2204	5.7	0.00–50.00
(13)	4.507	8.1	0.4328	3.8	0.1122	7.6	39.47–64.47	0.2221	6.5	26.32–76.32
(14)	4.733	13.5	0.4298	3.0	0.1174	12.6	7.89–32.89	0.2294	10.0	0.00–50.00
(15)	4.689	12.4	0.4376	4.9	0.1166	11.8	67.11–92.11	0.2302	10.4	50.00–100.00
(16)	5.445	30.5	0.4255[a]	2.0[a]	0.1275	22.3	75.00–100.00	0.2334	11.9	50.00–100.00

Discussion

Context and Performance of Screened Reactions

The results reported here are consistent with previous computational explorations of Diels–Alder reactions. Shi et al.[42] found previously that substitutions onto Diels–Alder diene molecules can cause changes (62.2% and 64.2%) in ΔH_{rxn}. These values are similar to the more significant changes observed in the substituted furan reactions (maximum 67.4%) and lend support to the idea that functional group substitution can be effective for tuning the reaction enthalpy. In addition, Boutelle and Northrop[43] specifically predicted changes in the Gibbs free energy of modified furan/maleimide reactions (ΔG ranging from -9.4 kcal mol^{-1} to 0.9 kcal mol^{-1}) where functional groups (including methyl, methoxy, and formyl groups) were substituted onto the furan 2 and 3 positions.

Kinetic Considerations

In this study, thermodynamic equilibrium was assumed for all calculations. However, for practical thermal storage applications, non-equilibrium properties are likely to be important. This study offers no information about the energy barriers to either the forwards or retro Diels–Alder reaction. Further calculations involving the transition states, energy barriers, and reaction rate constants should be conducted in the future to determine the practical reversibility of these reactions[44,45]. Predictions of reaction rates, as well as other dynamical properties such as thermal conductivity, will be of great use in the design of thermochemical storage systems using Diels–Alder reactions. We also emphasize that screening only on thermodynamic criteria, which is a necessary but not sufficient condition for a practical thermal fluid, already screens out roughly 90% of candidate reactions. Thus, a good portion of screening can be conducted through a thermodynamic analysis.

Many Diels–Alder reactions suffer from high reaction energy barriers, requiring high temperatures and long reflux periods in order to achieve appreciable chemical yield. However, there exist a number of Diels–Alder reactions with exceptionally low energy barriers. Such reactions have been used in dynamic covalent chemistry (DCC) at moderate temperatures and with fast rates.[46,47] Additionally, activated Diels–Alder reactions can be achieved by the addition

of a Lewis acid catalyst.[48,49] We expect that Reactions (1), (4), (8), and (9), as well as their functionally substituted counterparts, will not suffer from high energy barriers and poor kinetic behavior. Because the dienophiles involved in these reactions, namely crotonaldehyde, 2-methylpropenal, acrylonitrile, and maleimide, have strongly electron withdrawing groups (nitrile in the case of acrylonitrile, and carbonyl in the case of crotonaldehyde, 2-methylpropenal, and maleimide), the reactions should have sufficiently low energy barriers for applications in thermal energy storage and heat transfer. Diels–Alder reactions based on furan derivatives and maleimide derivatives with sufficiently low energy barriers for DCC applications have already been identified,[43] further supporting the idea that for such modified furan/maleimide reactions as (16), kinetic limitations should not be prohibitive. Moreover, Lewis acid catalysts can be identified to accelerate these reactions.

Recent experiments have focused on applications of thermally reversible Diels–Alder reactions for self-healing polymers. Liu and Chuo,[50] in their review on the topic, highlight the use of reactions based on the furan/maleimide system to achieve reversibly crosslinked polymer chains. Experimental results such as these, which have used moderate temperatures (80-150 °C) to achieve high healing efficiency in solid polymers (as high as 90%) suggest that thermal reversibility and even repeated thermal cycling should in principle be feasible for all-liquid Diels–Alder systems.

It should be noted that high reaction enthalpy ΔH_{rxn}, while desirable for its role in energy density, turning temperature, and heat capacity, could have a negative impact on reaction kinetics. The Bell-Evans-Polanyi principle[51,52] states that as ΔH_{rxn} increases within a particular class of reactions, the activation energy of the reaction increases. This suggests that a moderate reaction enthalpy change may be ideal in order to allow both the forwards and reverse reactions to proceed at reasonable rates.

Impact of Solvent

We have noted previously that water has an exceptional specific heat capacity, making it a strong choice for thermal energy storage for applications within its working temperature range. While organic solvents will, without exception, be able to contribute less sensible heat storage to a thermal fluid than water, they offer several benefits that merit their consideration. First, an organic solvent could allow for thermal energy storage applications outside of the working temperature range of water. A number of reactions have been identified in this screening study that exhibit significant heat capacity enhancements outside of the working range of water. Reactions such as 2-aminofuran/maleimide *exo,* 2-hydroxymethylfuran/maleimide *exo* (16), and 3-hydroxymethylfuran/maleimide *exo* appear to show promise for thermal transfer and storage at elevated temperatures (100–300 °C). The 2-aminofuran/acrylonitrile reaction, which shows elevated heat capacity at low temperatures, could be used in a refrigeration system if paired with a fluid with low melting point. Studying the thermodynamic and thermal properties of Diels–Alder reactions in different solvents could lead to a range of Diels–Alder-based thermal fluids that can be employed for different applications. Moreover, while functional group substitution has proven effective in improving the solubility of insoluble reactants, the work of Sparks and Poling[18] hints at even further gains in effective heat capacity that would be possible with more

soluble Diels–Alder reactants. It is reasonable to expect that high solubility could be achieved with organic solvents, potentially resulting in even higher heat capacities and energy storage densities than those predicted here.

Comparing Computational Methods

The less accurate opt-freq-sp(solv) calculations generally underestimate the values of ΔH_{rxn} and ΔS_{rxn} for the reactions examined when compared to the more accurate opt(solv)-freq(solv) workflow (see Table S.8.1 in the Supporting Information). On average for the 15 reactions analyzed with opt(solv)-freq(solv), ΔH_{rxn} for opt(solv)-freq(solv) was 16.3% more negative than for opt-freq-sp(solv), while ΔS_{rxn} was 2.1% more negative. The opt-freq-sp(solv) also underestimated the turning temperature in 14 of the 15 cases examined. In several cases, the more accurate opt(solv)-freq(solv) calculations clarify that reactions that initially showed promise based on the coarse opt-freq-sp(solv) workflow are most likely inappropriate for aqueous thermal storage. It should be noted that the turning temperatures of reactions (11) and (16) predicted by the opt(solv)-freq(solv) method are also slightly outside of the working temperature range of water. Although this limits the utility of reactions (11) and (16) for aqueous thermal storage applications, the gains in heat capacity and energy storage density are still considerable for these reactions.

While the lower computational demand of the opt-freq-sp(solv) workflow justifies its use for purposes of high-throughput screening, as it was used here, it is worth asking if the use of this method for pre-screening could have adversely affected which reactions were selected. We believe that this is not the case. Because there were no reactions that could have, by underestimation of T^*, been excluded from the set of potentially reversible reactions, it is unlikely that any reactions with actual turning temperature within the working range of water were overlooked during screening in this study. Nonetheless, we advise the use of more precise methods such as opt(solv)-freq(solv) whenever possible for future screening efforts. Such high-precision calculations, which directly incorporate the solvent environment, should also be used for analysis of Diels–Alder reaction pathways, kinetics, and stereoselectivity[53].

Future Work

In the computational screening by Kiyabu et al.,[24] the authors developed design rules based on select descriptors of the hydrates and hydroxides studied. Future work on Diels–Alder reactions could follow suit, developing a more thorough understanding of the physical principles underlying the properties of the cycloaddition reaction family and their suitability for thermal storage. Such design rules and descriptors could accelerate both computational and experimental selection of reactions for thermochemical storage and heat transfer.

The search space of Diels–Alder reactions for thermal storage and transfer applications has barely been explored. The test set used for this study should be expanded to include more reactions with a wider array of functional groups. Each of the potentially reversible reactions identified could be further analyzed as the cyclopentadiene/crotonaldehyde (1), cyclopentadiene/2-methylpropenal (4), furan/acrylonitrile (8), and furan/maleimide *exo* (9) reactions were; as we have shown, reaction systems with improved solubility and tunable ΔH_{rxn}

and T^* can be constructed through the addition of even simple functional groups. For those systems that already saw some functional group substitutions, the possibility exists to greatly expand the number and type of functional groups used. Multiple substitutions on the same reactant or simultaneous substitutions on both reactants could also yield novel and promising reactions.

Conclusions

In this study, we analyzed the thermodynamic properties of a set of Diels–Alder reactions to identify candidates with properties appropriate for use in aqueous thermochemical storage systems. From an initial test set of 52 reactions, we identified nine potentially reversible reactions with turning temperatures within the working temperature range of water. In addition to their favorable turning temperatures, several of these reactions demonstrated modest improvements in the heat capacity and energy density of water. We selectively modified four of the potentially reversible reaction with moderate solubility (the cyclopentadiene/crotonaldehyde, cyclopentadiene/2-methylpropenal, furan/acrylonitrile, and furan/maleimide *exo* reactions) through the addition of functional groups, generating 60 reactions that were not initially in the test set. Of these substitutions, several were predicted to show significantly elevated effective heat capacity within or near the working temperature range of water; we subjected these reactions to additional analysis with a more precise workflow, opt(solv)-freq(solv). Through this analysis, we have identified seven reactions (2-methylaminocyclopentadiene/crotonaldehyde, 2-aminocyclopentadiene/crotonaldehyde, 2-methylaminocyclopentadiene/2-methylpropenal, 2-aminocyclopentadiene/2-methylpropenal, 2-hydroxymethylfuran/acrylonitrile, 3-hydroxymethylfuran/acrylonitrile, and 2-hydroxymethylfuran/maleimide *exo*) with highly promising properties for thermal energy storage in a variety of applications. These reactions are predicted to enhance the maximum heat capacity of water by as much as 30.5%. Furthermore, they are predicted to improve the thermal energy density of water by as much as 22.3% over a 25°C range, 11.9% over a 50°C range, or 4.9% over the entire 100°C working temperature range of water. Experimental studies to validate the results of this study are ongoing.

Acknowledgments

This research was primarily supported by the Laboratory Directed Research and Development Program (LDRD) at Lawrence Berkeley National Laboratory under contract No. DE-AC02-05CH11231. Additional funding for E.W.C. Spotte-Smith was provided by the U.S. Department of Energy, Office of Science, Office of Workforce Development for Teachers and Scientists (WDTS) under the Science Undergraduate Laboratory Internship (SULI) program. This work used resources of the National Energy Research Scientific Computing Center, a DOE Office of Science User Facility supported by the Office of Science of the U.S. Department of Energy under Contract No. DE-AC02-05CH11231.

Author Contributions

EWCSS, PY, RSP, and AJ conceived of and designed the study. EWCSS, PY, and SMB performed the calculations. All authors contributed to writing the final manuscript.

---

[1] H. Inaba, *Int. J. Therm. Sci.* **2000**, *39*, 991-1003.
[2] H. Zhang, J. Baeyens, G. Cáceres, J. Degrève, Y. Lv, *Prog. Energy Combust. Sci.* **2015**, *53*, 1-40.
[3] P. H. Poole, F. Sciortino, T. Grande, H. E. Stanley, C. A. Angell, *Phys. Rev. Lett.* **1994**, *73*, 1632-1635.
[4] S. Pratt, *Proper fluid selection and maintenance for heat transfer applications*. Thermo Fisher Scientific, Newington, New Hampshire.
[5]J. Cot-Gores, A. Castell, L.F. Cabeza, *Renew. Sust. Energ. Rev.* **2012**, *16*(7), 5207-5224.
[6] C. Prieto, P. Cooper, A.I. Fernández, L.F. Cabeza, *Renew. Sust. Energ. Rev*. **2016**, *60*, 909-929.
[7] M.L. Mastroianni, B.E. Poling, *Thermochim. Acta.* **1982**, *53*(2), 141-147.
[8] M.A. Fahim, T.A. Al-Sahhaf, S.E.M. Hamam, *Int. J. Energ. Res*. **1989**, *13*(3), 289-296.
[9] M. Fischer, S. Bruzzano, B. Egenolf-Jonkmanns, B. Zeidler-Fandrich, H. Wack, G. Deerberg, *Energy Procedia*. **2014**, *48*, 327-336.
[10] P. Yu, A. Jain, R. S. Prasher, *Nanosc. Microsc. Therm.* **2019**, 1-12.
[11] O. Diels, K. Alder, *Justus Liebigs Annalen der Chemie.* **1928**, *460*(1), 98-122.
[12] M. A. Tasdelen, *Polym. Chem.* **2011**, *2*(10), 2133-2145.
[13] B. G. Sparks, P. F. Thompson, B. E. Poling, *AIChE Symposium Series.* **1981**, *77*.
[14] T. G. Lenz, L. S. Hegedus, J. D. Vaughan, *Int. J. Energ. Res*. **1982**, *6*, 357-365.
[15] W. L. Jorgensen, D. Lim, J. F. Blake, *J. Am. Chem. Soc*. **1993**, *115*, 2936-2942.
[16] N. Roy, J.-M. Lehn, *Chem. Asian J*. **2011**, *6*, 2419-2425.
[17] B. Egenolf-Jonkmanns, S. Bruzzano, G. Deerberg, M. Fischer, T. Marzi, M. Tyukavina, J. S. Gomez, H. Wack, B. Zeidler-Fandrich, *Energy Procedia.* **2012**, *30*, 235-243.
[18] B. Sparks and B. Poling, *AIChE J*. **1983**, *29*, 534-537.
[19] Q. Yan, J. Yu, S. K. Suram, L. Zhou, A. Shinde, P. F. Newhouse, W. Chen, G. Li, K. A. Persson, J. M. Gregoire, J. B. Neaton, *Proc. Natl. Acad. Sci. U.S.A.* **2017**, *114*(12), 3040-3043.
[20] X. Qu, A. Jain, N. N. Rajput, L. Cheng, Y. Zhang, S. P. Ong, M. Brafman, E. Maginn, L. A. Curtiss, K. A. Persson, *Comp. Mat. Sci*. **2015**, *103*, 56-67.
[21] S. Curtarolo, G. L. Hart, M. B. Nardelli, N. Mingo, S. Sanvito, O. Levy, *Nat. Mater.* **2013**, *12*, 191.
[22] A. Jain, Y. Shin, K. A. Persson, *Nat. Rev. Mater*. **2016**, *1*(1), 15004.
[23] H. B. Dizaji, H. Hosseini, *Renew. Sust. Energ. Rev.* **2018**, *98*, 9-26.
[24] S. Kiyabu, J. S. Lowe, A. Ahmed, D. J. Siegel, *Chem. Mater*. **2018**, *30*, 2006-2017.
[25] B. Sjoeberg, *Database Reaxys*.
[26] U.S. E.P.A. *Estimation Programs Interface Suite for Microsoft Windows, v 4.11*. **2012**.
[27] D. Weininger. *J. Chem. Inf. Comput. Sci*. **1988**, *28*(1), 31-36.
[28] S. P. Ong, W. D. Richards, A. Jain, G. Hautier, M. Kocher, S. Cholia, D. Gunter, V. L. Chevrier, K. A. Persson, G. Ceder, *Comp. Mat. Sci*. **2013**, *68*, 314-319.
[29] N. M. O'Boyle, M. Banck, C. A. James, C. Morley, T. Vandermeersch, G. R. Hutchison, *J. Cheminformatics*. **2011**, *3*, 33.
[30] N. M. O'Boyle, C. Morley, G. R. Hutchison, *Chem. Cent. J*. **2008**, *2*, 5.

[31] Y. Shao, Z. Gan, E. Epifanovsky, A. T. Gilbert, M. Wormit, J. Kussmann, A. W. Lange, A. Behn, J. Deng, X. Feng, et al., *Mol. Phys*. **2015**, *113*, 184-215.
[32] J.-D. Chai, M. Head-Gordon, *Phys. Chem. Chem. Phys*. **2008**, *10*, 6615-6620.
[33] P.C. Hariharan, J. Pople, *Mol. Phys.* **1974**, *27*(1), 209-214.
[34] P. D. Mezei, G. I. Csonka, M. Kallay, *J. Chem. Theory Comput*. **2015**, *11*, 2879-2888.
[35] R. B. J. S. Krishnan, J. S. Binkley, R. Seeger, J. A. Pople, *J. Chem. Phys.* **1980**, *72*, 650-654.
[36] E. Cances, B. Mennucci, J. Tomasi, *J. Chem. Phys*. **1997**, *107*, 3032-3041.
[37] D. Feller, K. Schuchardt, D. Jones. *Extensible Computational Chemistry Environmental Basis Set Database (Version 1.0)*. **2000**.
[38] A. V. Marenich, C. J. Cramer, D. G. Truhlar, *J. Phys. Chem. B*. **2009**, *113*, 6378-6396.
[39] K. Mathew, J. H. Montoya, A. Faghaninia, S. Dwarakanath, M. Aykol, H. Tang, I.-h. Chu, T. Smidt, B. Bocklund, M. Horton, et al., *Comp. Mat. Sci*. **2017**, *139*, 140-152.
[40] A. Jain, S. P. Ong, W. Chen, B. Medasani, X. Qu, M. Kocher, M. Brafman, G. Petretto, G.-M. Rignanese, G. Hautier, et al., *Concurr. Comp-Pract. E*. **2015**, *27*, 5037-5059.
[41] A. Hagberg, P. Swart, D. S. Chult, *Proceedings of the 7th Python in Science conference (SciPy 2008).* **2008**, 11-15.
[42] Z. Shi, W. Liang, J. Luo, S. Huang, B. M. Polishak, X. Li, T. R. Younkin, B. A. Block, A. K.-Y. Jen, *Chem. Mater*. **2010**, *22*, 5601-5608.
[43] R. C. Boutelle and B. H. Northrop, *J. Org Chem*. **2011**, *76*, 7994-8002.
[44] T. S. Khan, S. Gupta, M. I. Alam, M. A. Haider, *RSC Adv*. **2016**, *6*(103), 101697-101706.
[45] G. O. Jones, V. A. Guner, K. N. Houk, *J. Phys. Chem. A*. **2006**, *110*(4), 1216-1224.
[46] P. J. Boul, P. Reutenauer, J. M. Lehn, *Org. Lett.* **2005**, *7*(1), 15-18.
[47] F. Li, X. Li, X. Zhang, *Org. Biomol. Chem.* **2018**, *16*(42), 7871-7877.
[48] S. Otto, F. Bertoncin, J. B. Engberts, *J. Am. Chem. Soc.* **1996**, *118*(33), 7702-7707.
[49] F. Fringuelli, O. Piermatti, F. Pizzo, L. Vaccaro, *Eur. J. Org. Chem.* **2001**, *2001*(3), 439-455.
[50] Y.-L. Liu, T.-W. Chuo, *Polym. Chem*. **2013**, *4*, 2194-2205.
[51] R. P. Bell, *Proc. R. Soc. A*. **1936**, *154*, 414.
[52] M. G. Evans, M. Polanyi, *J. Chem. Soc. Faraday Trans*. **1936**, *32*, 1333.
[53] S. Kong, J. D. Evanseck, *J. Am. Chem. Soc*. **2000,** *122*, 10418-10427.